


Sustainable replacement of EDTA–Biojarosite for commercial iron in the Fenton’s and UV–Fenton’s degradation of Rhovedamine B – a process optimization using Box–Behnken method

Bhaskar S ^{a,*}, K. N. Rashmishree^a, B. Manu^a and M. Y. Sreenivasa^b

^a Department of Civil Engineering, National Institute of Technology Karnataka, Surathkal, P.O. Srinivasnagar, Mangalore 575025, India

^b Department of Studies in Microbiology, University of Mysore, Mysuru, Karnataka 570006, India

*Corresponding author. E-mail: baskarmalwanitk@gmail.com

 BS, 0000-0002-0203-3629

ABSTRACT

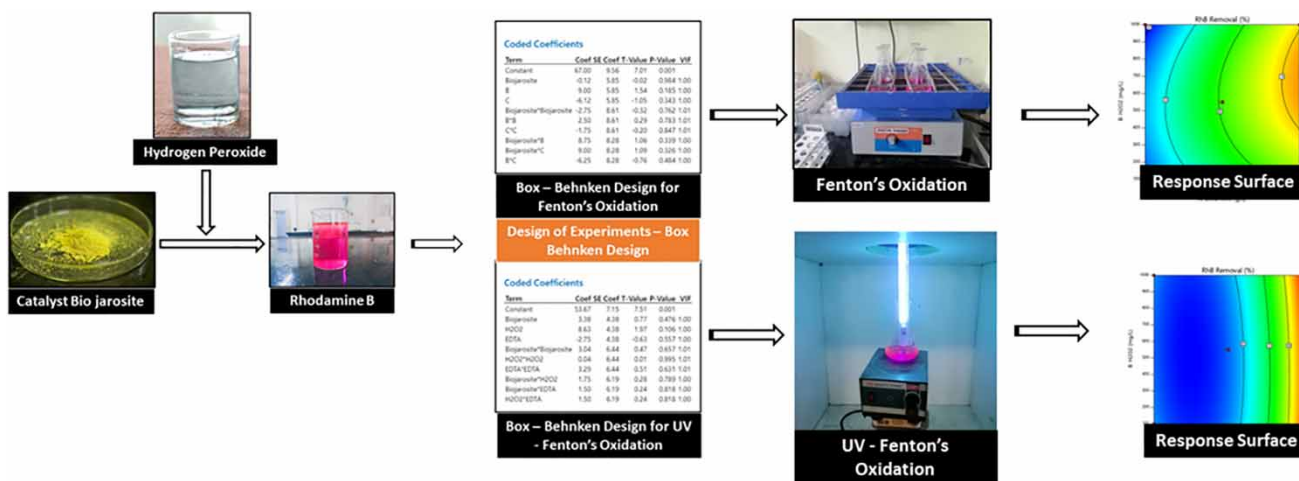
Biojarosite as a replacement for commercial iron catalyst in the oxidative degradation of the dye Rhodamine B was confirmed and established. Investigations on the oxidative degradation by Fenton’s oxidation and UV–Fenton’s oxidation with EDTA at neutral pH were conducted and degradation of target compound was evaluated. UV–Fenton’s oxidation was shown to be efficient over Fenton’s oxidation in the degradation of Rhodamine B with removal efficiency of 90.0%. Design of Experiments was performed with Box–Behnken design. Investigation was conducted for the predicted values separately for both Fenton’s oxidation and UV–Fenton’s oxidation and the Rhodamine B removal was taken as response. Variable parameters biojarosite, H₂O₂ dosage and EDTA were optimized in the range of 0.1–1 g/L, 2.94–29.4 mM and 10–100 mM, respectively. A quadratic regression model is fitted for both Fenton’s and UV–Fenton’s oxidation. Analysis of variance (ANOVA) is performed and model fit is discussed.

Key words: Box–Behnken, Biojarosite, EDTA, Fenton’s Process, Rhodamine B, UV–Fenton’s process

HIGHLIGHTS

- Biojarosite – EDTA based Fenton’s Oxidation.
- Biojarosite – EDTA based UV Fenton’s Oxidation.
- Process optimization – Box Behnken method.
- Commercial iron replacement from Biojarosite.
- Comparison of Fenton’s and UV–Fenton’s oxidation for degradation of Rhodamine B.

GRAPHICAL ABSTRACT



INTRODUCTION

Rapid development in the textile industries demands the usage of diverse chemical reagents, which leads to the generation of wastewater contaminated with environmental persistent chemicals. Dyes by the virtue of their nature are non-amenable to degradation on exposure to water and other chemicals (Dutta & Mukhopadhyay 2001). Xanthene dyes are widely used in textile industries and as fluorescent, among which Rhodamine B has a vast application in textile industries (Su *et al.* 2013). Dyes usually have benzene and naphthalene rings but may also contain aromatic or aliphatic groups. It is the side group attached to dye which imparts the color. It is the complex nature of dyes that make them more interesting in the field of chemical remediation. Discharge of wastewater containing dye to natural streams and rivers may harm the biodiversity posing toxicity to aquatic life (Islam & Mostafa 2018).

Many treatment methods like adsorption, biological degradation, filtration process and advanced oxidation have been tried over a decade by various researchers. Nanocomposites-based advanced oxidation process with metal oxides have been attempted in recent years claiming high removal efficiency with reduction in treatment time. Carbon iron-graphene oxide nano-composite based sono-Fenton's oxidation and iron doped carbon gel based electro Fenton's oxidation are efficient in organic compound removal with 99% organic carbon removal (Hassani *et al.* 2017; Ahmadi *et al.* 2021; Karim *et al.* 2022). Xue *et al.* (2009), studied the effect of ferrous and ferric on sorption and Fenton's like degradation of Rhodamine B and claimed efficiency of Fenton's oxidation increases with increase in H_2O_2 dosage or with exposed surface area (Xue *et al.* 2009). AlHamedi *et al.* (2009) investigated degradation of Rhodamine B in presence of UV light and claimed its high efficiency in the dye degradation. The team derived low molecular weight aliphatic alcohols and acids as the degradation products and observed the degradation follows first order linear kinetics (AlHamedi *et al.* 2009). Ozonation, electrochemical method, and photochemical methods have been suggested for dye degradation, out of which photochemical method is proven to be effective because of its application (Dong & Tang 1993; Kim *et al.* 2004; Huang *et al.* 2008). Hydroxyl peroxide produced on the dissociation of hydrogen peroxides acts on the complex structure of organic dyes, breaking it and causing the degradation. OH radicals formed act as initiators for the degradation as well as scavengers (Zhou *et al.* 2016). High dosage of reactants and catalyst leads to increasing the treatment cost. It is thus necessary to optimize the oxidation process for the degradation of any organic compounds. Studies on the replacement of commercial iron with lateritic iron in Fenton's oxidation have been conducted, and it was reported to cut down the cost of catalyst (Karale *et al.* 2014; Sangami & Manu 2018; Bhaskar *et al.* 2021). Bhaskar *et al.* (2019), biologically synthesized jarosite using novel *Acidithiobacillus ferrooxidans* strain and presented the application of synthesized biojarosite as a Fenton's catalyst in the degradation of Ametryn (Bhaskar *et al.* 2019). Apart from the catalyst and reactant dosage, a narrow range of acidic pH imposes another restriction on Fenton's oxidation.

Box-Behnken design (BBD) is a 3 interlocking 2^2 factorial design with points on the surface of a sphere surrounding the center of the design (Tripathi *et al.* 2009). BBD is used to optimize and investigate the influence of key process parameters as independent variables on the response as a dependent variable (Tak *et al.* 2015; Shokri *et al.* 2019). Being most suitable for chromatographic optimization of analysis, BBD indicates most significant factors and reveals many mutual interactions between the variable parameters (Ahmadi *et al.* 2017).

The present study encompasses novel replacement of commercial iron with biojarosite as a catalyst for the Fenton's and UV-Fenton's oxidation of Rhodamine B using EDTA as chelating agent. BBD is adopted for the optimization in which catalyst loading, H_2O_2 dosage and chelating agent concentration are taken as independent variables and rhodamine B removal efficiency is taken as response to fit the regression model.

MATERIALS AND METHODS

UV Fenton's and Fenton's oxidation of Rhodamine B

UV-Fenton's and Fenton's degradation of Rhodamine B was carried out with initial dye concentration of 5 mg/L for both the experiments (Zhao & Zhu 2006; Su *et al.* 2013). UV-Fenton's oxidation was carried out in a closed UV chamber with continuous stirring of solution in magnetic stirrer at an illumination of 254 nm with an intensity at the center of the solution being 5.6 mW/cm^2 . The experimental set-up is shown in Figure 1. Synthesis and characterization of Biojarosite were discussed earlier (Bhaskar *et al.* 2019). Biojarosite was added as per design dose into Rhodamine B solution separately taken in a conical flask. The solution was adjusted to pH 7 using 1 N H_2SO_4 or 1 N NaOH and allowed for 50 minutes to ensure proper mixing and uniform distribution of Biojarosite powder in the solution before addition of H_2O_2 . Initial investigation was conducted with 0.5 g/L of Biojarosite, 2.94 mM of H_2O_2 dosage and 50 mM of EDTA to ensure the degradation of Rhodamine B with Fenton's and UV-Fenton's oxidation before the run of design of experiments (DOE). Experimentation was as per design with a set of experimental conditions for both UV-Fenton's and Fenton's process separately. Samples were drawn at regular intervals for analysis. During sampling, each time 1 mL of sodium thiosulphate was added to arrest the reaction (Khan *et al.* 2009). Concentration of Rhodamine B was measured using double beam UV-Vis spectrophotometer. Chemical oxygen demand (COD) was measured using closed reflux calorimetric method (Lapara *et al.* 2000). pH was measured using digital pH meter. Ferric iron was measured by potassium thiocyanate method using UV-Vis spectrophotometer (Woods & Mellon 1941). H_2O_2 was measured using double beam UV-spectrophotometer (Eisenberg 1943).

Design of experiments – Box-Behnken design

Response surface methodology using BBD is adopted for the present study. BBD method was used in the present study. Response as the removal of Rhodamine B was analyzed via response surface methodology. Three levels (-1, 0, +1) were selected as independent variables and Rhodamine B removal was considered as dependent variable. 15 experimental runs were executed. The variable parameters were optimized in the range of 0.1 g/L to 1 g/L for Biojarosite, 2.94 mM to 29.4 mM for H_2O_2 dosage and 10–100 mM for EDTA concentration, and Rhodamine B is considered as response. Experimental data were fitted to regression model and 3D contour graphs were used to evaluate the optimized parameters which influence the responses (See Table 1).

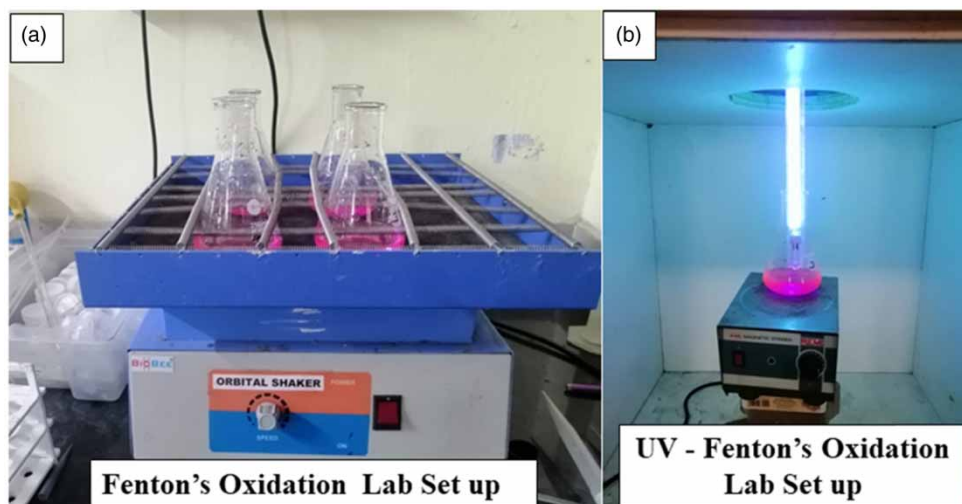


Figure 1 | Experimental Set-up for Fenton's and UV-Fenton's Oxidation of Rhodamine B.

Table 1 | Experimental levels of the variables

Dependent variables	Low Level (-1)	Mid-Level (0)	High Level (+1)
Biojarosite (g/L)	0.1	0.5	1.0
H ₂ O ₂ (mM)	2.94	16.17	29.4
EDTA (mM)	10	50	100

RESULTS AND DISCUSSION

Fenton's oxidation and UV-Fenton's oxidation of Rhodamine B

UV-Fenton's oxidation is found to be most effective for the removal of Rhodamine B in the current study. High removal efficiency of 91.0% was observed with the Biojarosite:H₂O₂ ratio of 5:1 and 50 mM EDTA addition. For Fenton's oxidation, about 70.0% of degradation was observed within 120 minutes of treatment and almost complete degradation within 40 minutes with a rate constant 0.01895/min on 0.5 g/L of catalyst loading. Increase in catalyst load is more beneficial than increasing hydrogen peroxide since iron increases the speed of the reaction (Lojo-López *et al.* 2021). For UV-Fenton's oxidation, about 60.0% of degradation was observed within first 40 minutes of treatment and 27.6% of degradation was observed in another 40 minutes on a catalyst load of 0.5 g/L with a rate constant 0.0629/min. Degradation of rhodamine B via Fenton's oxidation and UV-Fenton's oxidation is presented in Figure 2.

About 120 mg/L of leached iron out of Biojarosite has participated in the Fenton's and UV-Fenton's oxidation. There is an increase in the ferric form of iron at initial stage as leached iron gets oxidized to ferric form and later there is a drop in the concentration of ferric form of iron in the solution. The rate of oxidation depends on the dissolution rate of ferrous ion that has leached out from the jarosite. Initial dissolution of ferrous ions is consumed and the rate of reaction will be more. It is the amount of catalyst addition which indicates the adsorption part of this heterogenous Fenton's and UV-Fenton's oxidation that in turn contributes to maximum removal of target compounds in the process. Observed results are consistent with previous works (Bhaskar *et al.* 2019, 2021; Bhaskar & Basavaraju Manu 2020). On UV-Fenton's oxidation, high removal efficiency is correlated to photo reduction of formed ferric iron species (Arslan & Tuhkanen 1999; Tekbas *et al.* 2008). From Figure 2, it is observed that maximum removal is observed within 20 mins of the treatment with UV-Fenton's oxidation, which is attributed to photo reduction on the surface of Biojarosite. Bel *et al.* (2014) demonstrated non-catalytic UV based phenol degradation and Fe clay based UV based catalytic degradation of organic compounds (Bel *et al.* 2014). Iron leached

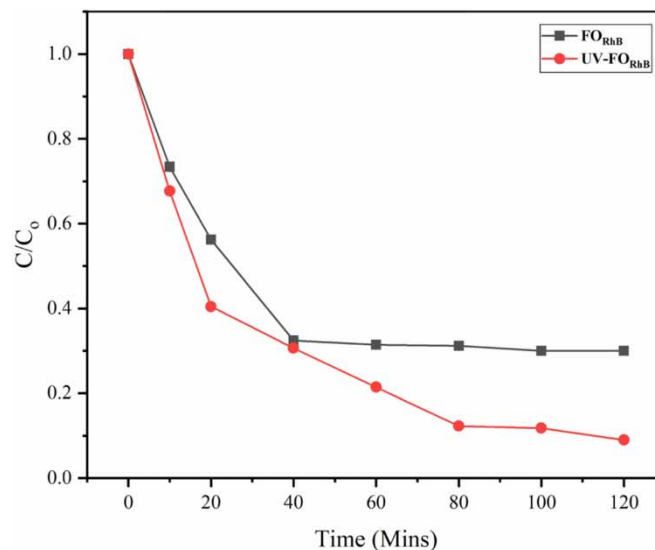


Figure 2 | Degradation of Rhodamine B on Fenton's and UV-Fenton's oxidation with 0.5 g/L of catalyst loading, 100 mg/L of H₂O₂ dosage and 500 mM of EDTA addition.

out of Biojarosite actively participated in Fenton's oxidation by the oxidation from ferrous to ferric form. Ferric iron reduced back to ferric in presence of UV light, which increases the dissociation of hydrogen peroxide to form hydroxyl radicals. OH radicals thus formed attacks the xanthene ring of rhodamine, initiating degradation.

In both Fenton's oxidation system and UV-Fenton's oxidation system, on addition of EDTA, an organic complex is formed at neutral conditions and increases the solubility of ferric iron in solution, limiting the ferric precipitation. This mechanism was observed by the previous works (Huang *et al.* 2008; Zhou *et al.* 2014; Tang *et al.* 2019). Regeneration of Fe-II EDTA complex accelerates the generation of OH radicals, promoting degradation.

Organic carbon removal was determined by the COD measurements in the present study. Maximum reduction in COD observed was 57.0% and 69.0% for the optimum removal of Rhodamine B via Fenton's oxidation and UV-Fenton's oxidation, respectively. Reduction in COD indicates better oxidation of target compound via both processes (Figure 3). The reduction in COD is also attributed to the adsorption process other than Fenton's oxidation (Masomboon *et al.* 2009).

Many researchers have discussed the degradation mechanism of Rhodamine B via Fenton's oxidation. Rhodamine B is susceptible to oxidation by the decomposition of the conjugated xanthene ring (Zhao & Zhu 2006). Degradation of Rhodamine B follows N-de-ethylation, chromophore cleavage, ring opening and mineralization stages. Zhou *et al.* (2016) identified three intermediate products due to de-ethylating steps of N,N'-diethylammonium groups such as N,N,N'-triethyl rhodamine, N,N'-diethyl rhodamine and rhodamine (Zhou *et al.* 2016). Hou *et al.* (2011) claim oxalic acid, formic acid and acetic acid as chromophore cleavage and ring opening intermediates. Tertiary amines formed during the degradation can be oxidized to amine oxides, which are further oxidized to aldehyde intermediates and then to carboxylic acids (Hou *et al.* 2011).

Catalytic efficiency of Biojarosite on reuse is tabulated in Table 2. Degradation on first cycle of reuse was 68.2% and 86.0% with rate constants 0.009/min and 0.0141/min for Fenton's oxidation and UV-Fenton's oxidation, respectively, while on second cycle of reuse the efficiency was 67.6% and 82.8% with rate constants 0.010/min and 0.0135/min, respectively. For the third cycle of reuse degradation efficiency was 65.6% and 82.4% with rate constants 0.009/min and 0.0127/min, respectively.

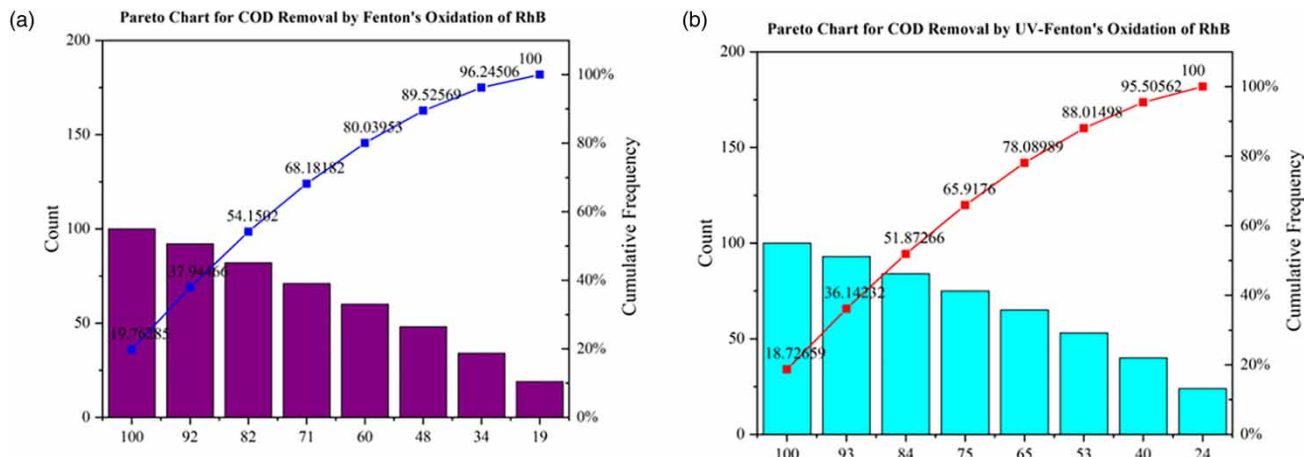


Figure 3 | Pareto chart for COD Removal on degradation of Rhodamine B. (a) Fenton's (b) UV-Fenton's Oxidation with 0.5 g/L of catalyst loading, 100 mg/L of H₂O₂ dosage and 500 mM of EDTA addition.

Table 2 | Reusability of catalyst on Fenton's and UV-Fenton's oxidation of Rhodamine B

Cycle	Fenton's oxidation		UV- Fenton's oxidation	
	k/min	R ²	k/min	R ²
1	0.0090	0.9701	0.0141	0.97653
2	0.0099	0.97816	0.0135	0.95436
3	0.0091	0.9052	0.0127	0.96835
4	0.0092	0.92416	0.0129	0.95889

Degradation on fourth cycle was 65.2% and 82.6% with rate constants 0.009/min and 0.0129/min, respectively (Figure 4). The degradation efficiency was found to be constant after third consecutive cycle of the catalyst, marking the limit for reuse.

Fenton's oxidation and UV-Fenton's oxidation of Rhodamine B – design optimization

Model F-value 89.80 indicates that the model is significant for the Rhodamine B removal by Fenton's oxidation. There is only 0.01% chance that F-value could occur due to noise. Probability value of <0.0001 indicates that the model is significant. A regression co-efficient $R^2 = 0.9939$ is a measure of goodness of fit of the model, indicating there is a high degree of correlation between observed value and predicted value. The value suggests that more than 99.39% of variance is attributed to variables showing high significance for Fenton's oxidation of Rhodamine B model. Only 0.61% of total variance cannot be explained by the model. The analysis of variance (ANOVA) quadratic regression model demonstrated that the model was highly significant for Fenton's oxidation of Rhodamine B with a low probability ($p < 0.0001$) in the F-test and an insignificant contribution from lack of fit of the model. The F - value of 0.75 for lack of fit implies that lack of fit does not contribute significantly to the total error. There is a 61.48% chance that a lack of fit F-value this large could occur due to noise. The predicted R^2 value of 0.9414 is in reasonable agreement with adjusted R^2 value 0.9828, i.e., the difference is less than 0.2.

For UV-Fenton's oxidation, the model F-value 69.21 indicates that the model is significant for the Rhodamine B removal by UV-Fenton's oxidation. There is only a 0.01% chance that this F- value could occur due to noise. Probability value of <0.0001 indicates that the model is significant. A regression co-efficient $R^2 = 0.9920$ is a measure of goodness of fit of the model, indicating that there is a high degree of correlation between observed value and predicted value. The value suggests that more than 99.20% of variance is attributed to variables showing high significance for UV-Fenton's oxidation of Rhodamine B model. Only 0.80% of total variance cannot be explained by the model.

The ANOVA quadratic regression model demonstrated that the model was highly significant for UV-Fenton's oxidation of Rhodamine B with a low probability value ($p < 0.0001$) in the F-test and insignificant contribution from lack of fit of the model. A lack of fit F-value of 7.75 implies that lack of fit is not significant in relation to pure error. There is a 11.64% chance that a lack of fit F-value this large could occur due to noise. The predicted R^2 value of 0.8813 is in reasonable agreement with adjusted R^2 value 0.9777, i.e., the difference is less than 0.2.

Co-efficient of variance (CV) obtained in the model for Fenton's oxidation is 2.47%; hence, the model can be considered to be reproducible. The CV value indicates high precision and reliability of the experiments. The p values of regression co-efficient suggest that among the independent test variables linear, quadratic and interaction effect the Fenton's oxidation of Rhodamine B and are highly significant. For UV-Fenton's oxidation, co-efficient of variance obtained in the model is 3.41%; hence, the model can be considered to be reproducible. The CV value indicates high precision and reliability of

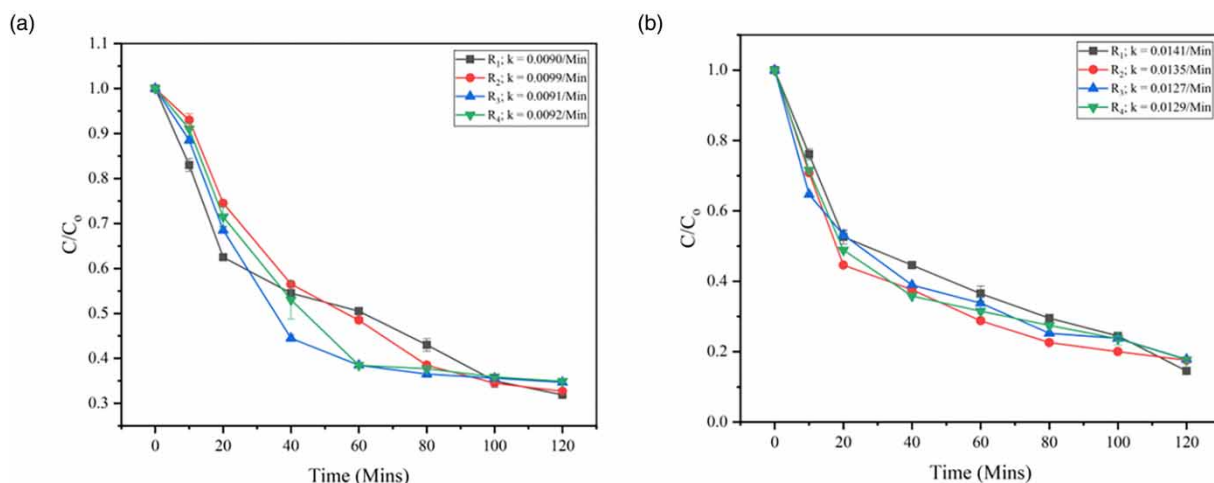


Figure 4 | Reusability of catalyst for the degradation of Rhodamine B. (a) Fenton's Oxidation (b) UV-Fenton's Oxidation with 0.5 g/L of catalyst loading, 2.94 mM of H_2O_2 dosage and 500 mM of EDTA addition.

the experiments. The p values of regression co-efficient suggest that among the independent test variables, there are linear, quadratic and interaction effects on the Fenton's oxidation of Rhodamine B, which are highly significant.

In the present study, A, C, AB and B² are significant model terms for the Fenton's oxidation of Rhodamine B. Thus, statistical analysis of all the experimental data showed that Biojarosite loading, H₂O₂ dosage and EDTA concentration had a significant effect on Fenton's oxidation. It is observed that Biojarosite loading and EDTA dosage exerted more linear influence on Fenton's oxidation, which indicates that Rhodamine B removal by the process was positively influenced by Biojarosite loading, H₂O₂ dosage and addition of EDTA. Higher positive linear effect of iron dosage over H₂O₂ in Fenton's oxidation had been reported by the researchers in previous work. Again, Biojarosite loading has the highest positive linear

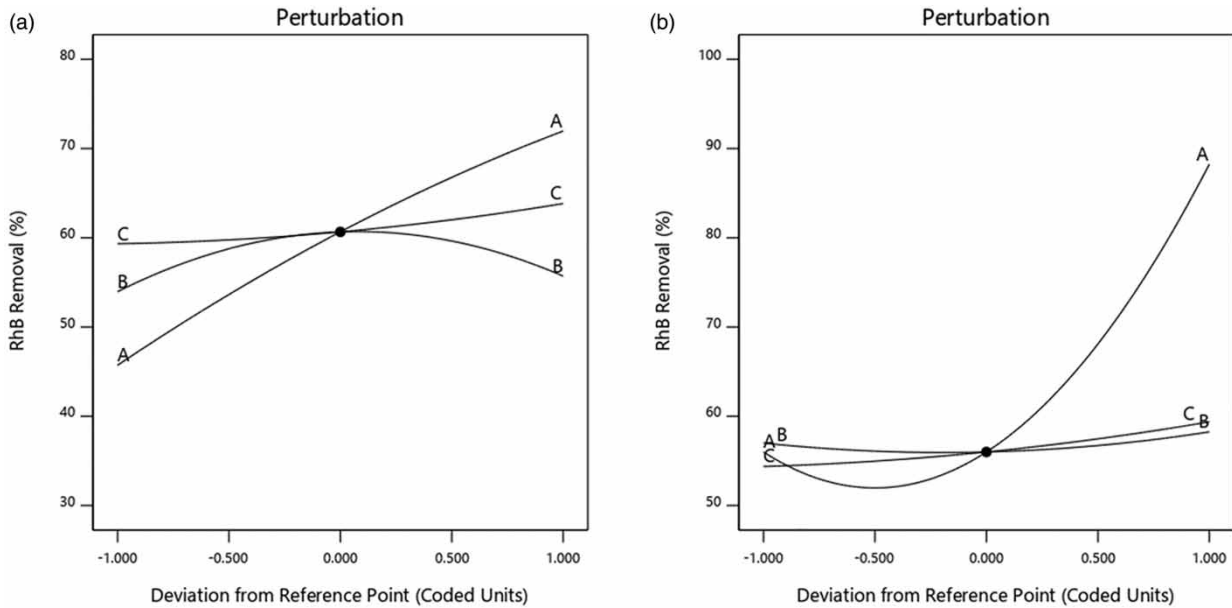


Figure 5 | Perturbation plot for the degradation of Rhodamine B. (a) Fenton's Oxidation (b) UV-Fenton's Oxidation.

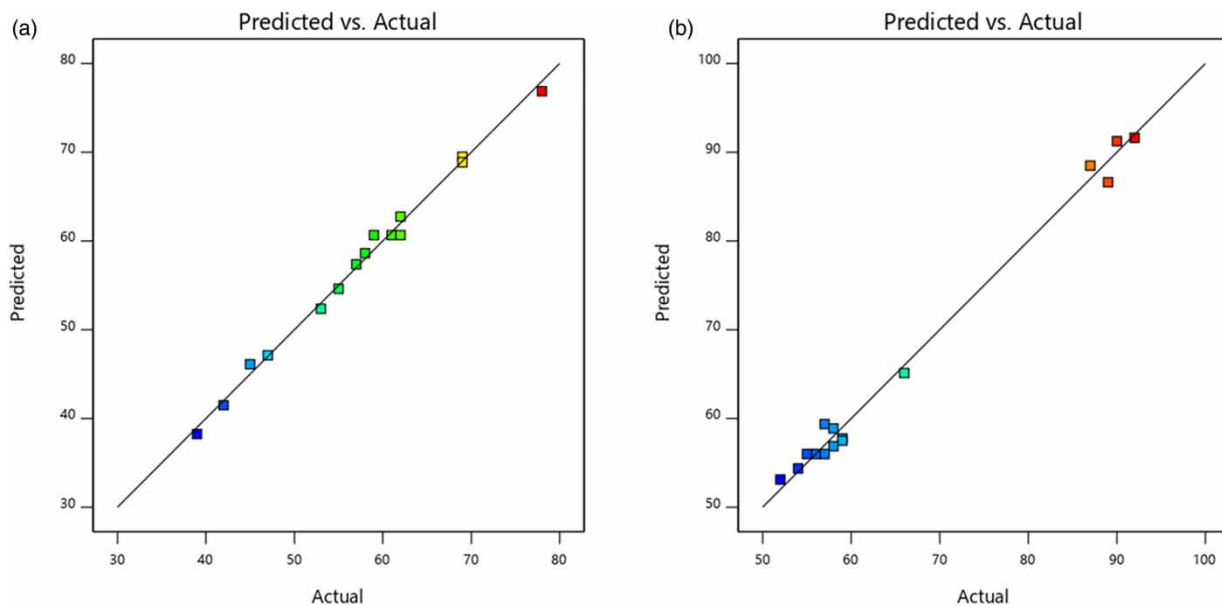


Figure 6 | Prediction and actual response for the degradation of Rhodamine B. (a) Fenton's Oxidation (b) UV-Fenton's Oxidation.

influence (high co-efficient) than influence of EDTA. The quadratic effect of the independent variables on Fenton’s oxidation of Rhodamine B was negative.

The linear regression quadratic equation of the model fit is explained by

$$Y = 60.67 + 13.12A + 0.87B + 2.25C + 2.5AB + 1.75AC - 0.25BC - 1.83A^2 - 5.83B^2 + 0.916C^2.$$

A, C, BC and A² are significant model terms for the UV–Fenton’s oxidation of Rhodamine B. Thus, statistical analysis of all the experimental data showed that Biojarosite loading and EDTA addition had a significant effect on UV–Fenton’s oxidation. It is observed that Biojarosite loading and EDTA dosage exerted more linear influence on UV–Fenton’s oxidation, which indicates that Rhodamine B removal by the UV–Fenton’s oxidation was positively influenced by Biojarosite loading and addition

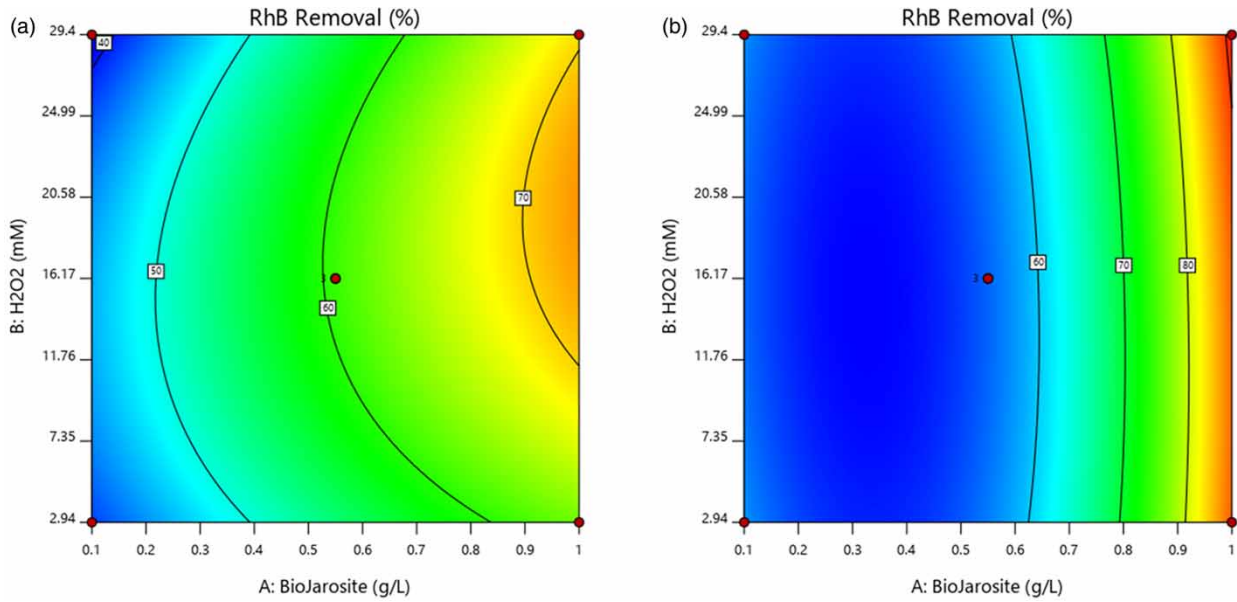


Figure 7 | Contour plot for the degradation of Rhodamine B. (a) Fenton’s Oxidation (b) UV–Fenton’s Oxidation.

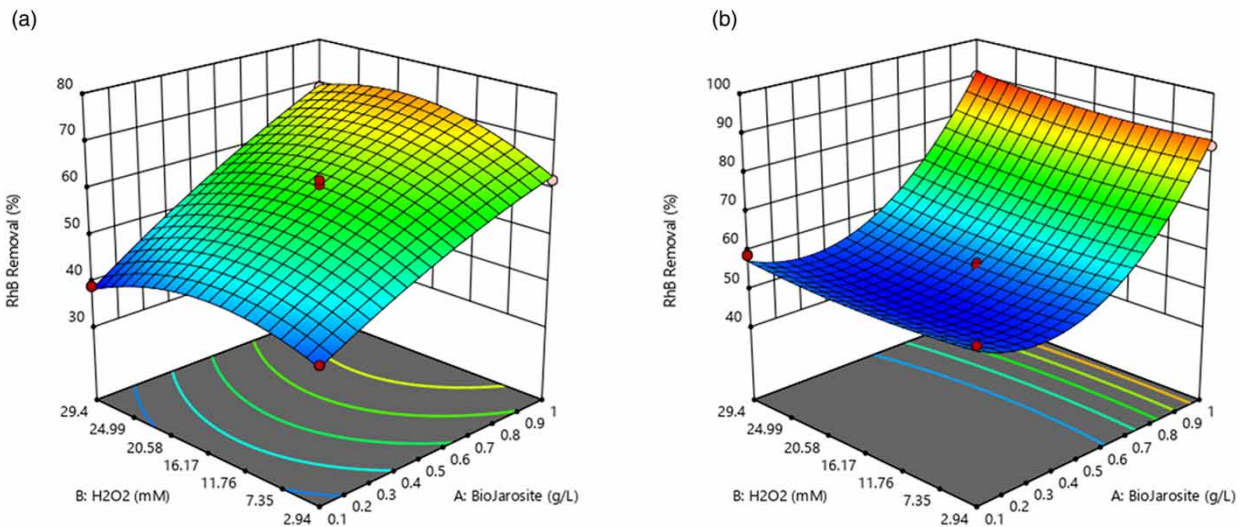


Figure 8 | Response surface plot for the degradation of Rhodamine B. (a) Fenton’s Oxidation (b) UV–Fenton’s Oxidation.

of EDTA. Again, Biojarosite loading has a higher positive linear influence (16.12) than influence of EDTA concentration (2.50). The quadratic effect of the independent variables on Fenton’s oxidation of Rhodamine B was negative.

The linear regression quadratic equation of the model fit is explained by

$$Y = 56.00 + 16.12A + 0.625B + 2.5C + 0.75AB + 3.5BC + 16.13A^2 + 1.63B^2 + 0.875C^2.$$

In comparison with Fenton’s oxidation, UV-Fenton’s oxidation has all the co-efficients like interaction, linear and quadratic positive, while in the Fenton’s oxidation all the interaction and linear co-efficients are positive and the three quadratic

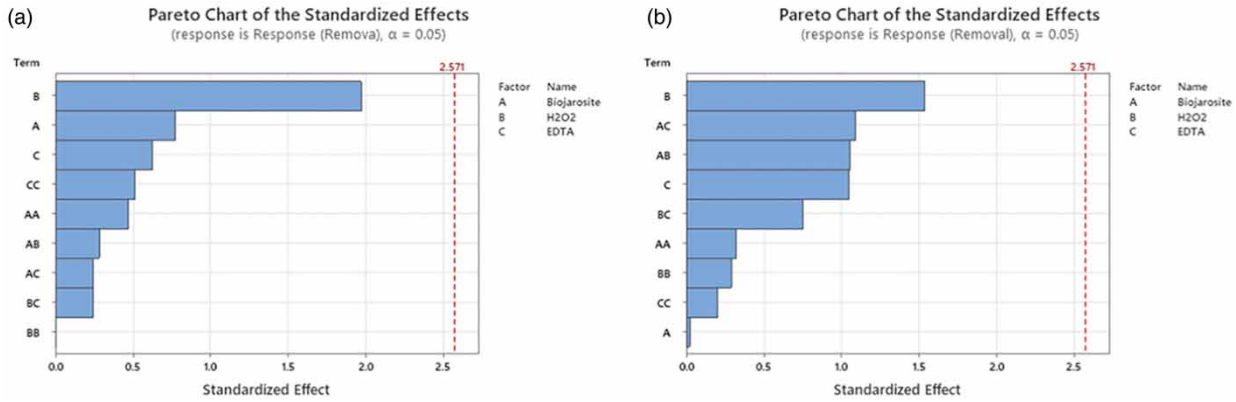


Figure 9 | Pareto chart for response on degradation of Rhodamine B. (a) Fenton’s Oxidation (b) UV-Fenton’s Oxidation.

Table 3 | ANOVA for the quadratic response surface model fitting for Fenton’s oxidation of Rhodamine B

	SS	df	MS	F-value	p-value	Remarks
Residual Model	1,603.02	9	178.11	89.80	<0.0001	Significant
Lack of fit	5.25	3	1.75	0.75	0.6148	Not significant
Pure error	4.67	2	2.33			
Total correlation	1,612.93	14				

R² = 0.9939.
 Adjusted R² = 0.9828.
 Predicted R² = 0.9414.
 Adequate Precision = 33.5905.

Table 4 | Co-efficient of the model for Fenton’s oxidation of Rhodamine B

Factor	Co-efficient estimate	Standard error	F-value	p-value	Remarks
X	60.67	0.81	89.80	<0.0001	Significant
A	13.12	0.49	694.85	<0.0001	Significant
B	0.875	0.49	3.09	0.1392	Not significant
C	2.25	0.49	20.42	0.0063	Significant
AB	2.50	0.70	12.61	0.016	Significant
AC	1.75	0.70	6.18	0.055	Significant
BC	-0.25	0.70	0.12	0.737	Not significant
A ²	-1.83	0.73	6.26	0.054	Significant
B ²	-5.83	0.73	63.35	0.005	Significant
C ²	0.9167	0.73	1.56	0.266	Not significant

co-efficients are negative. Figure 5 shows a perturbation plot in which response is plotted over rhodamine removal over Biojarosite loading, H₂O₂ dosage and EDTA concentration 0.55, 550 and 55 as actual factors. Actual and predicted response for both Fenton's oxidation and UV-Fenton's oxidation are highly relevant (Figure 6). From Figure 7 it is observed that Fenton's oxidation for Rhodamine B removal works in a narrow range of Biojarosite and H₂O₂ dosage, while UV-Fenton's oxidation has a comparatively broad range. Figure 8 shows 3D response surface plot for Fenton's oxidation and UV-Fenton's oxidation.

Influence of independent variables on dependent variables was analyzed using Pareto chart (Figure 9). In case of Fenton's oxidation, B (H₂O₂ dosage), A (Biojarosite dosage) and C (EDTA concentration) have the significant effects, while for UV-Fenton's oxidation, B (H₂O₂ dosage), AC (Combinational effect of Biojarosite and EDTA), AB (Combinational effect of Biojarosite and H₂O₂), C (EDTA concentration) and BC (Combinational effect of H₂O₂ and EDTA concentration) have significant effects. In both the cases, H₂O₂ dosage was shown to have highest effect (See Tables 3–7).

Table 5 | ANOVA for the quadratic response surface model fitting for UV-Fenton's oxidation of Rhodamine B

	SS	df	MS	F-value	p-value	Remarks
Residual Model	3,145.68	9	349.52	69.21	0.0001	Significant
Lack of fit	23.25	3	7.75	7.75	0.1164	Not significant
Pure error	2.00	2	1.00			
Total correlation	3,170.93	14				

R² = 0.9920.

Adjusted R² = 0.9777.

Predicted R² = 0.8813.

Adequate Precision = 20.9827.

Table 6 | Co-efficient of the model for UV-Fenton's oxidation of Rhodamine B

Factor	Co-efficient estimate	Standard error	F-value	p-value	Remarks
X	56	1.30	69.21	0.0001	Significant
A	16.12	0.7945	411.91	<0.0001	Significant
B	0.6250	0.7945	0.6188	0.4671	Not significant
C	2.50	0.7945	9.90	0.0255	Significant
AB	0.75	1.12	0.4455	0.5340	Not significant
AC	0.00	1.12	0	1.00	Not significant
BC	3.5	1.12	9.70	0.0264	Significant
A ²	16.13	1.17	190.11	<0.0001	Significant
B ²	1.63	1.17	1.93	0.2234	Not significant
C ²	0.8750	1.17	0.5598	0.4880	Not significant

Table 7 | Overview of Fenton's and UV-Fenton's oxidation of Rhodamine B optimized with Box-Behn design

Method	Biojarosite:H ₂ O ₂	EDTA (mM)	RhB removal (%)
UV-Fenton's Oxidation	1:1	55	90.0
Fenton's Oxidation	1:0.55	100	78.0

CONCLUSIONS

Fenton's oxidation and UV-Fenton's oxidation for the degradation of Rhodamine B using synthesized Biojarosite as a catalyst and EDTA as chelating agent at neutral pH were optimized with model fitting using Box-Behnken design. Initial investigation with Biojarosite and EDTA reveals that UV-Fenton's oxidation is more efficient in the degradation of Rhodamine B. Actual response over predicted response on Box-Behnken method was analyzed and both the model is fitted the actual response with a high degree of precision. Influencing parameters in the model for both methods are discussed and a quadratic equation is derived. The study claims that both Fenton's oxidation and UV-Fenton's oxidation work effectively for the degradation of dye Rhodamine B, and Biojarosite can be used as a replacement for the commercial iron catalyst at neutral pH using EDTA.

DATA AVAILABILITY STATEMENT

All relevant data are included in the paper or its Supplementary Information.

CONFLICT OF INTEREST

The authors declare there is no conflict.

REFERENCES

- Ahmadi, M., Rahmani, K., Rahmani, A. & Rahmani, H. 2017 Removal of benzotriazole by Photo-Fenton like process using nano zero-valent iron: response surface methodology with a Box-Behnken design. *Polish Journal of Chemical Technology* **19** (1), 104–112.
- Ahmadi, A., Zarei, M., Hassani, A., Ebratkhahan, M. & Olad, A. 2021 Facile synthesis of iron (II) doped carbonaceous aerogel as a three-dimensional cathode and its excellent performance in electro-Fenton degradation of ceftazidime from water solution. *Separation and Purification Technology* **278**, 119559. <https://doi.org/10.1016/j.seppur.2021.119559>.
- AlHamed, F. H., Rauf, M. A. & Ashraf, S. S. 2009 Degradation studies of Rhodamine B in the presence of UV/H₂O₂. *Desalination* **239** (1–3), 159–166. <https://doi.org/10.1016/j.desal.2008.03.016>.
- Arslan, I. & Tuhkanen, T. 1999 Oxidative treatment of simulated dyehouse effluent by UV and near UV light assisted Fenton's reagent. *Chemosphere* **39** (15), 2767–2783.
- Bel, H., Da, P., Beaunier, P., Elena, M. & Ben, M. 2014 Fe-clay-plate as a heterogeneous catalyst in photo-Fenton oxidation of phenol as probe molecule for water treatment. *Applied Clay Science* **91–92**, 46–54. <https://doi.org/10.1016/j.clay.2014.01.020>.
- Bhaskar, S. & Basavaraju Manu, M. Y. S. 2020 Green synthesis of Bioleached Flyash Iron Nanoparticles (GBFFeNP) using *Azadirachta indica* leaves and its application as Fenton's catalyst in the degradation of dicamba. In: *Recent Trends in Civil Engineering* Springer, pp. 365–371.
- Bhaskar, S., Manu, B. & Sreenivasa, M. Y. 2019 Bacteriological synthesis of iron hydroxysulfate using an isolated *Acidithiobacillus ferrooxidans* strain and its application in ametryn degradation by Fenton's oxidation process. *Journal of Environmental Management* **232**, 236–242. <https://doi.org/10.1016/j.jenvman.2018.11.048>.
- Bhaskar, S., Manu, B. & Sreenivasa, M. Y. 2021 Bioleaching of iron from laterite soil using an isolated *Acidithiobacillus ferrooxidans* strain and application of leached laterite iron as Fenton's catalyst in selective herbicide degradation. *PLoS ONE* **16**. <https://doi.org/10.1371/journal.pone.0243444>.
- Dong, C. P. H. C. & Tang, Z. 1993 Advanced chemical oxidation: its present role and potential future in hazardous waste treatment. *Waste Management* **13**, 361–377.
- Dutta, K. & Mukhopadhyay, S. 2001 Chemical oxidation of methylene blue using a Fenton-like reaction. *Journal of Hazardous Materials* **84**, 57–71.
- Eisenberg, G. M. 1943 Colorimetric determination of hydrogen peroxide. *Industrial and Engineering Chemistry* **15** (5), 327–328.
- Hassani, A., Çelikdağ, G., Eghbali, P., Sevim, M., Karaca, S. & Metin, Ö. 2017 Reduced graphene oxide (CoFe₂O₄-rGO) nanocomposite for the removal of organic dyes from aqueous solution. *Ultrasonics – Sonochemistry*. <https://doi.org/10.1016/j.ultsonch.2017.08.026>.
- Hou, M., Liao, L., Zhang, W., Tang, X., Wan, H. & Yin, G. 2011 Degradation of rhodamine B by Fe (0)-based Fenton process with H₂O₂. *Chemosphere* **83** (9), 1279–1283. <https://doi.org/10.1016/j.chemosphere.2011.03.005>.
- Huang, Y., Huang, Y., Chang, P. & Chen, C. 2008 Comparative study of oxidation of dye-Reactive Black B by different advanced oxidation processes: Fenton, electro-Fenton and photo-Fenton **154**, 655–662. <https://doi.org/10.1016/j.jhazmat.2007.10.077>.
- Islam, M. R. & Mostafa, M. G. 2018 Textile dyeing effluents and environment concerns – a review. *Journal of Environmental Science and Natural Resources* **11**, 131–144.
- Karale, R. S., Manu, B. & Shrihari, S. 2014 Fenton and Photo-Fenton oxidation processes for degradation of 3-Aminopyridine from water. *APCBEE Procedia* **9**, 25–29. <https://doi.org/10.1016/j.apcb.2014.01.005>.
- Karim, A. V., Hassani, A., Eghbali, P. & Nidheesh, P. V. 2022 Nanostructured modified layered double hydroxides (LDHs) -based catalysts: a review on synthesis, characterization, and applications in water remediation by advanced oxidation processes. *Current Opinion in Solid State & Materials Science* **26** (1), 100965. <https://doi.org/10.1016/j.cossms.2021.100965>.

- Khan, E., Wirojanagud, W. & Sermsai, N. 2009 Effects of iron type in Fenton reaction on mineralization and biodegradability enhancement of hazardous organic compounds. *Journal of Hazardous Materials* **161**, 1024–1034. <https://doi.org/10.1016/j.jhazmat.2008.04.049>.
- Kim, T., Park, C., Yang, J. & Kim, S. 2004 Comparison of disperse and reactive dye removals by chemical coagulation and Fenton oxidation. *Journal of Hazardous Materials* **112**, 95–103. <https://doi.org/10.1016/j.jhazmat.2004.04.008>.
- Lapara, T. M., Alleman, J. E. & Pope, P. G. 2000 Miniaturized closed reflux, colorimetric method for the determination of chemical oxygen demand. *Waste Management* **20**, 295–298.
- Lojo-López, M., Andrades, J. A., Egea-Corbacho, A., Coello, M. D. & Quiroga, J. M. 2021 Degradation of simazine by photolysis of hydrogen peroxide Fenton and photo-Fenton under darkness, sunlight and UV light. *Journal of Water Process Engineering* **42**, 102115. <https://doi.org/10.1016/j.jwpe.2021.102115>.
- Masomboon, N., Ratanatamskul, C. & Lu, M. C. 2009 Chemical oxidation of 2, 6-Dimethylaniline in the Fenton process. *Environmental Science & Technology* **43** (22), 8629–8634.
- Sangami, S. & Manu, B. 2018 Catalytic efficiency of laterite based FeNPs for the mineralization of mixture of herbicides in water. *Environmental Technology*, 1–30. <https://doi.org/10.1080/09593330.2018.1449899>.
- Shokri, A., Bayat, A. & Mahanpoor, K. 2019 Employing Fenton-like process for the remediation of petrochemical wastewater through Box–Behnken design method. *Desalination and Water Treatment* **166**, 135–143. <https://doi.org/10.5004/dwt.2019.24634>.
- Su, S., Guo, W., Leng, Y., Yi, C. & Ma, Z. 2013 Heterogeneous activation of oxone by $\text{CO}_x\text{Fe}_3\text{O}_4$ nanocatalysts for degradation of rhodamine B. *Journal of Hazardous Materials* **244–245**, 736–742. <https://doi.org/10.1016/j.jhazmat.2012.11.005>.
- Tak, B., Tak, B., Kim, Y., Park, Y., Yoon, Y. & Min, G. 2015 Optimization of color and COD removal from livestock wastewater by electrocoagulation process: application of Box–Behnken design (BBD). *Journal of Industrial and Engineering Chemistry* **28**, 307–315.
- Tang, Y., Liu, H., Zhou, L., Ren, H., Li, H., Zhang, J., Chen, G. & Qu, C. 2019 Enhanced Fenton-like oxidation of hydroxypropyl guar gum catalyzed by EDTA-metal complexes in a wide pH range. *Water Science and Technology*, 1667–1674. <https://doi.org/10.2166/wst.2019.169>.
- Tekbas, M., Yatmaz, H. C. & Bektas, N. 2008 Heterogeneous photo-Fenton oxidation of reactive Azo dye solutions using iron exchanged zeolite as a catalyst Mesut Tekbas. *Microporous and Mesoporous Materials* **115**, 594–602. <https://doi.org/10.1016/j.micromeso.2008.03.001>.
- Tripathi, P., Chandra, V. & Kumar, A. 2009 Optimization of an azo dye batch adsorption parameters using Box–Behnken design. *Desalination* **249** (3), 1273–1279. <https://doi.org/10.1016/j.desal.2009.03.010>.
- Woods, J. & Mellon, M. 1941 Thiocyanate method for iron: a spectrophotometric study. *Industrial & Engineering Chemistry Analytical Edition* **13** (8), 551–554.
- Xue, X., Hanna, K. & Deng, N. 2009 Fenton-like oxidation of Rhodamine B in the presence of two types of iron (II, III) oxide. *Journal of Hazardous Materials* **166**, 407–414. <https://doi.org/10.1016/j.jhazmat.2008.11.089>.
- Zhao, X. U. & Zhu, Y. 2006 Synergetic degradation of Rhodamine B at a porous ZnWO_4 film electrode by combined electro-oxidation and photocatalysis. *Environmental Science & Technology* **40** (10), 3367–3372.
- Zhou, H., Sun, Q., Wang, X., Wang, L., Chen, J., Zhang, J. & Lu, X. 2014 Removal of 2, 4-dichlorophenol from contaminated soil by a heterogeneous ZVI/EDTA/air Fenton-like system. *Separation and Purification Technology* **132**, 346–353. <https://doi.org/10.1016/j.seppur.2014.05.037>.
- Zhou, W., Zhao, H., Gao, J., Meng, X. & Qin, Y. 2016 Influence of a reagents addition strategy on the Fenton oxidation of Rhodamine B: control of the competitive reaction of OH. *RSC Advances* **6** (3), 108791–108800. <https://doi.org/10.1039/c6ra20242j>.

First received 3 August 2022; accepted in revised form 10 September 2022. Available online 3 October 2022